Spectral line broadening using ABO theory

Adam Hultquist

Advisor: Paul Barklem

Uppsala University, Department of Physics and Astronomy, Astronomy and Space physics

Advanced Physics - Project Course, 10 credits

January, 2019

Abstract

Having knowledge of the behaviour of spectral lines is of great importance in stellar spectroscopy. In particular the collisional broadening of spectral lines will be considered. Collisional broadening is a type of spectral broadening which occurs when a particle collides into another particle which is in the process of emitting or absorbing a photon. This project aims to continue on previous work by extending the calculations to silicon and titanium. These will be calculated using ABO theory. The goal is that these results can then be of use for further stellar spectral analysis in the Gaia – ESO survey.

1 Background

1.1 The Gaia - ESO survey project

The Gaia – ESO survey is a public spectroscopic survey that covers more than 10^5 stars in many parts of the Milky Way. The data is of importance for the understanding of the composition and evolution of the Milky Way, as well as other problems in stellar physics. This projects aims to calculate the collisional line broadening of spectral lines in solar type stars observed by the Gaia-ESO survey, which is used to determine the abundance of various elements in these types of stars.

1.2 Spectral line broadening

A stellar spectral line is an irregularity, bright or dark band, in the otherwise continuous radiation from the star. These peaks and valleys are created when a photon is absorbed and emitted by elements in the stellar atmospheres and effectively creates a "fingerprint" for the atoms and molecules in the star. This band also experiences an amount of broadening around its central wavelength. This broadening can have several causes. First of all the uncertainty in energy and lifetime of a emission/absorption are related via the uncertainty principle. A shorter lifetime is associated with a larger uncertainty in energy. Mathematically this can be seen as the uncertainty principle

$$\Delta E \Delta t \geq \frac{h}{4\pi} \tag{1.1}$$

For small values of Δt the ΔE would be large. This type of broadening, which is always present, is called natural broadening and results in a Lorentzian shape of the spectral line. The type of broadening this project is focused on is the collision broadening. Collision broadening, sometimes called pressure broadening, is caused by a atom or molecule, called a perturber, colliding with a particle that is in the process of emitting or absorbing a photon. For fast collisions, this causes a shortening of the lifetime and thus a larger uncertainty in energy. This then leads to further line broadening. For stellar atmospheres the temperatures are often high enough (which means large particle velocities) that the interaction is short compared to the normal timescale for the photon emission. This is, in essence, what the impact approximation means, that the interaction is far shorter than normal de-excitation time. For example, if a titanium atom is perturbed by a hydrogen atom during the absorption of a photon, the resulting line will be broadened because of this process. In stellar atmospheres with temperatures close to that of our sun hydrogen is the dominant perturber in the atmosphere. Therefore this model can be used effectively (Anstee, Barklem and O'Mara, 1998).

1.3 The ABO theory

The ABO theory is a modern theory for calculating cross sections and is a successor of the previous Unsold theory which is based on the ideas of Lindholm (Anstee, Barklem and O'Mara, 1998). The strength of the Unsold theory however, was in its simplicity of use, which kept it prevalent for a long time. Compared to earlier methods the ABO theory can calculate the line broadening per perturber more accurately than the Unsöld theory, which is usually only correct up to a factor of 2. This is essential for a more complete understanding of the composition of stellar atmospheres.

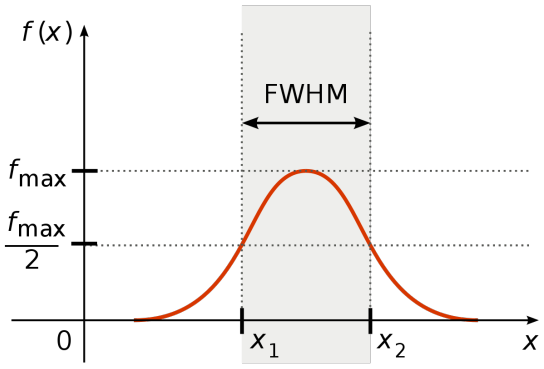

Figure 1: An illustration of a FWHM

One of the strengths in this method is that it only requires the Coulomb wavefunction, which can be described with only a few parameters. These parameters are the species, wavelength of the line, the energies for both states of the emitter, series limits as well as the L

and J quantum numbers for the optical electron. In the end the J quantum number is not used for calculation but is still included for the sake of completeness. Using these parameters as input the ABO cross code then computes the cross section of interaction (written as σ) and the velocity parameter (written as α) which are then used to find the width per perturber. The cross section is the area in which the particles must be for there to be an interaction, an analogy for this could be how a dart must hit the dart board for a point to be registered. This is a simplification though, since the cross section in reality is a integrated property that reflects various probabilities.

The cross section and velocity parameters can be found manually using the tables made by (Anstee, S. O'Mara, B, 1995) and (Barklem and O'Mara, 1997) or through linear regression with the ABO cross code. First the effective principle quantum numbers are calculated (written as n^*). This can be calculated as

$$n^* = \sqrt{\frac{109678.8}{E_{limit} - E_{nl}}}$$

Here E_{lim} is the series limit, which is explained in a later part, and E_{nl} is the energy of the optical electron. This then means that their difference $E_{lim} - E_{nl}$ is the binding energy of the electron and 109678,8 is the Rydberg constant in $[cm^{-1}]$. These effective quantum numbers can then be used to find the σ and α in tables by (Anstee, S. O'Mara, B, 1995) and (Barklem and O'Mara, 1997).

The calculated values of the $\frac{w}{N}$ are written in a somewhat different form when done by the code. They are output as

$$log\left(\frac{\Gamma}{N}\right) \quad \text{where} \quad \Gamma = \frac{FWHM}{N} = \frac{2w}{N}$$

This output is properly understood by observing figure 1. While $\frac{w}{N}$ describes the width per perturber the full width is the twice that broadening. This means that the FWHM (full width half maximum), which can be seen in figure 1, is actually $2w$, or in the context of the output, $\frac{FWHM}{N} = \frac{2w}{N}$.

When the data has all been gathered and double checked it is converted into to a text document to be used in the ABO code. After use of the ABO - cross code the results come in .short and .long format. The .long format is used, since it contains more data. The data comes out in the parameters

1. Species (The name of the element. For example, Si or Ti)
2. Ionization stage (Indicates how many electrons that have been ionized. Neutral Si is Si I)
3. Wavelength (λ of the transition. Measured in Ångström)
4. E_{low} (The energy for the lower state in cm^{-1})
5. E_{limit} (The series limit for the lower state in cm^{-1})
6. E_{upp} (The energy of the upper state in cm^{-1})
7. E_{limit} (The series limit of the upper state in cm^{-1})
8. l (The azimuthal quantum number of the transition)
9. J (The total angular momentum quantum number of the transition)
10. n_{low} (The effective principal quantum number of the lower state)
11. n_{upp} (The effective principal quantum number of the upper state)
12. Sigma (σ) (The cross section area, in $(Bohr\ radius)^2 = a_0^2$
13. Alpha (α) (The velocity parameter)
14. $log\left(\frac{FWHM}{N}\right)$ (The calculated values according to ABO theory. in cgs units)
15. $log\left(\frac{FWHM}{N}\right)$ (The calculated values according to Unsold theory, in cgs units)

This data is the converted back to a excel spreadsheet to then be used by the Matlab program provided by (Bengtsson, K, 2018).

1.4 The series limit

For all of the calculations made in this project the series limit (written E_{limit}) and the ionization energy (written E_{ion}) are needed. The series limit is the highest possible level an electron can have without becoming ionized. The expression $(E_{lim} - E_{nl})$ is the binding energy, which makes sense since the ionized electron has no binding energy when $E_{nl} = E_{limit}$. In the traditional case where only the optical electron is excited, meaning that the parent atomic core is in its ground state, the series limit is the same as the ionization limit. If another core electron is in an excited state however, the resulting E_{limit} is shifted up and the energy of the parent core state is added to the E_{ion}. This process requires knowledge of the parent configurations term symbol. Once the term symbol is determined its energy can be found on NIST and then added to the E_{ion}. In short in can be summarized as

$$E_{limit} = E_{ion} + E_{parent\ configuration}$$

2 Method

2.1 Computing the series limit

Since the series limit has a central role in the method it is necessary to know how to properly compute it. The parent configuration is an important aspect of the series limit. The parent configuration is the atom that is left after the optical electron has been ionized. For example for the configuration $3s2.3p.4p$ (3D') the optical electron is in the state $4p$. So once ionized gives a parent configuration of $3s2.3p$. In this case the term symbol initially was $3D'$ and a $4p$ electron was removed. The spin multiplicity is computed $2S + 1$ where S is total spin and the $4p$ electron has a total spin of $1/2$ the new total spin is either $1/2$ more or less than previously, depending on its orientation. This results in a new spin multiplicity of 2 or 4. The $4p$ electron also has a orbital angular quantum number $l = 1$ and the 3D' term symbol means $L = 2$. This gives three possibilities for the new letter in the term symbol

$$|L - l|, |L - (l + 1)|, \ldots , |L + l| \rightarrow |2 - 1|, |2|, |2 + 1|$$

Which means it could be 1(P), 2(D) or 3(F). In this case however, the only possible term symbol for the $3s2.3p$ is $2P$ which is a relief since it is one of the possible ones. This state also corresponds to the ground state, which has an energy of zero relative to itself. It can be noted that this energy is zero *over* ground state. This energy is then added to the ionization energy. This gives a series limit which is equal to the ionization limit.

In other cases, it might not be so clear how it should be done. For the state $3s.3p3$ 3D*' the optical electron is a $3p$ electron and the initial term symbol is $3D*'$. Once ionized the state becomes $3s.3p2$ with the possible L – values of 1(P), 2(D), 3(F) with possible spins S = 2 or 4. When compared to the possible values on NIST the state $3s.3p2$ can have the term symbols 4P, 2D, 2S and 2P. Out of these four, three are possible. In certain cases (for the d4 to d3 core configuration) tables of the probabilities of the states can be used to create a weighted average and in other cases the arithmetic mean is computed instead. For this project it was decided to compute with both the term symbol corresponding to the lowest energy and the average of the energies of the possible states. The implications of this are discussed later. For this example they can be written

$$E_{lim_{4P}} = 108558.48\ [cm^{-1}] \quad \text{and} \quad E_{lim_{avg}} = 130287.075\ [cm^{-1}]$$

Once all the series limits had been computed they were stores in an excel spreadsheet and then converted into a text file for use with the ABO – code. For the cases where there several ways to compute the series limit (as above) the line was included twice in the code. The second inclusion of the line was the "weighted" line and the first one the lowest energy option.

3 Calculations

3.1 Important constants

Several constants are used during the calculations in accordance to the cgs (centimeter - gram - second) system.

$$u = 1.660539040(20) \cdot 10^{-24}\ [g] \quad \text{(The atomic unit mass)}$$

$$k = 1.380 \cdot 10^{-16}\ [erg K^{-1}] \quad \text{(The Boltzmann constant)}$$

$$R = 109678.8\ [cm^{-1}] \quad \text{(The Rydberg constant)}$$

$$v_0 = 10^6\ [cms^{-1}] \quad \text{(Assumed initial velocity)}$$

3.2 Equations

$$n^* = \sqrt{\frac{109678.8}{E_{limit} - E_{nl}}} \tag{3.1}$$

$$\overline{v} = \sqrt{\frac{8kT}{\pi\mu}} \tag{3.2}$$

$$\frac{w}{N} = \left(\frac{4}{\pi}\right)^{\frac{\alpha}{2}} \Gamma\left(\frac{4-\alpha}{2}\right) v_0 \sigma(v_0) \left(\frac{\overline{v}}{v_0}\right)^{1-\alpha} \tag{3.3}$$

$$\mu = \frac{m_1 m_2}{m_1 + m_2} \tag{3.4}$$

3.3 P − S transition of Ti I with $\lambda = 4978,1875$ [Å]

To illustrate how this method can be used practically a couple of examples have been calculated by hand. For this transition the corresponding energies for the lower and higher states (written E_{low} and E_{up}) can be found on NIST by their respective configurations. Relative to the ground state of Ti I they are:

$$E_{low} = 15881\ [cm^{-1}] \quad E_{up} = 35956\ [cm^{-1}] \quad E_{lim_{low}} = 55072\ [cm^{-1}] \quad E_{lim_{up}} = 55072\ [cm^{-1}]$$

For titanium it is sometimes the case that the parent configuration of the atom is not excited, which means that the $E_{lim} = E_{ion}$. This is the case for both states in this situation. Using equation 3.1 n^*_{low} and n^*_{up} can then be calculated

$$n^*_{low} = 1.672 \approx 1.7 \quad \text{and} \quad n^*_{up} = 2.395 \approx 2.4$$

The cross section and velocity parameter can now by found in the tables provided by (Anstee, S. O'Mara, B, 1995) and (Anstee, Barklem and O'Mara, 1997). Because of how the tables are constructed it is convenient to round the numbers when doing calculation by hand. The reduced mass can also be computed according to equation 3.4. These are computed to be

$$\sigma = 790\ [in\ a_0^2] \quad \text{and} \quad \alpha = 0.235 \quad \text{and} \quad \mu = 0.95\ [atomic\ units]$$

The mean velocity is also needed to continue. This can be computed with equation 3.2 and the assumption that $T = 5000\ [K]$ like Anstee and O'Mara (1995)

$$\overline{v} = \sqrt{\frac{8kT}{\pi\mu}} = 1.487 \cdot 10^6\ [cms^{-1}]$$

Once these values have been determined they can be used in equation 3.3

$$\frac{w}{N} = \left(\frac{4}{\pi}\right)^{\frac{0.235}{2}} \Gamma\left(\frac{4-0.235}{2}\right) 10^6 \cdot 790 \cdot 2.8 \cdot 10^{-17} \left(\frac{1.052 \cdot 10^6}{10^6}\right)^{1-0.235} = 2.9453 \cdot 10^{-8} \; [rad \cdot s^{-1} \cdot cm^3]$$

This line has no published value but when the same line is calculated with the ABO - cross code it gives the value

$$\frac{w}{N} = 2.9105 \cdot 10^{-8} \; [rad \cdot s^{-1} \cdot cm^3]$$

Which is a 1.1 percent difference.

3.4 S − P transition of Na I with $\lambda = 5895.92$ [Å]

In a very similar fashion to the example above this transition can be calculated by hand. In this case, however, there is a published result to compare by. The line can be found on NIST and the following data is acquired

$$E_{low} = 0 \; [cm^{-1}] \quad E_{up} = 16956 \; [cm^{-1}]$$

As well as the electron configurations and corresponding term symbols. In this case the lower configuration is 2p6.3s (2S) and the upper is 2p6.3p (2P'). Once ionized these both yield the parent configuration 2p6 (1S) since it is the only possibility. This state also corresponds to the ground state of Na II which means that

$$E_{limit_{low}} = E_{limit_{upp}} = E_{ion} = 41449 \; [cm^{-1}]$$

Now, using equation 3.1 the effective principle quantum numbers can be computed

$$n^*_{low} = 1.626 \approx 1.6 \quad \text{and} \quad n^*_{up} = 2.116 \approx 2.1$$

Now that the effective quantum number have been computed and rounded the resulting cross section and velocity parameters can be found in the tables by (Anstee, S. O'Mara, B, 1995) and (Anstee, Barklem and O'Mara, 1997) just like above

$$\sigma = 396 \quad \alpha = 0.283$$

Now that all the important quantities are gathered the temperature is again assumed to be 5000 $[K]$ and equation 3.3 is used

$$\frac{w}{N} = \left(\frac{4}{\pi}\right)^{\frac{0.283}{2}} \Gamma\left(\frac{4-0.283}{2}\right) 10^6 \cdot 396 \cdot 2.8 \cdot 10^{-17} \left(\frac{1.052 \cdot 10^6}{10^6}\right)^{1-0.283} = 1.142 \cdot 10^{-8} \; [rad \cdot s^{-1} \cdot cm^3]$$

This result can then be compared to the published result of

$$\frac{w}{N} = 1.167 \cdot 10^{-8}$$

Which is a difference of just over 2 percent. So the method used with the calculations appear to agree with earlier published data fairly well.

4 Results

4.1 Tables

Spec	Ion	$Wavel$	E_{low}	$E_{limit_{low}}$	E_{upp}	$E_{limit_{upp}}$	L	J	n^*_{low}	n^*_{upp}	σ	α	ABO	$Kurucz$
Ti	1	4978.188	15881.166	55072.500	35956.445	55072.500	1->0	2.0->1.0	1.673	2.395	788.61	0.231	-7.235	-7.604
Ti	1	5062.102	17421.696	67553.823	37174.350	67553.823	0->1	2.0->1.0	1.479	1.900	306.46	0.248	-7.648	-7.939
Ti	1	5064.060	21736.792	55072.500	41481.381	55072.500	1->2	5.0->4.0	1.814	2.841	689.58	0.301	-7.306	-7.597
Ti	1	5064.060	21736.792	57351.118	41481.381	55072.500	1->2	5.0->4.0	1.755	2.841	702.78	0.305	-7.298	-7.591
Ti	1	5230.967	18058.878	64781.667	37174.350	67553.823	0->1	1.0->1.0	1.532	1.900	316.03	0.241	-7.634	-7.974
Ti	1	5429.137	18913.832	64781.667	37327.597	67553.823	0->1	2.0->2.0	1.546	1.905	320.32	0.242	-7.628	-7.979
Ti	1	5440.509	11533.808	55932.777	29907.245	55932.777	0->1	2.0->2.0	1.572	2.053	374.08	0.262	-7.564	-7.852
Ti	1	5448.907	18825.110	64781.667	37174.350	67553.823	0->1	1.0->1.0	1.545	1.900	318.55	0.242	-7.631	-7.984
Ti	1	5449.150	11638.661	55932.777	29987.901	55932.777	0->1	3.0->3.0	1.574	2.056	375.51	0.264	-7.563	-7.850
Ti	1	5465.773	8605.995	64815.472	26890.710	63578.161	0->1	2.0->3.0	1.397	1.729	247.63	0.246	-7.741	-8.091
Ti	1	5465.773	8605.995	68125.805	26890.710	63578.161	0->1	2.0->3.0	1.357	1.729	241.34	0.246	-7.752	-8.053
Ti	1	5511.779	11775.776	55932.777	29915.310	70108.503	0->1	4.0->3.0	1.576	1.652	255.37	0.260	-7.730	-8.073
Ti	1	5514.343	11533.808	55932.777	29665.277	55072.500	0->1	2.0->1.0	1.572	2.078	383.55	0.273	-7.555	-7.834
Ti	1	5514.533	11638.661	55932.777	29770.130	55072.500	0->1	3.0->2.0	1.574	2.082	385.48	0.275	-7.554	-7.831
Ti	1	5565.474	18034.682	67577.732	35996.773	63578.161	0->1	4.0->4.0	1.488	1.994	340.08	0.243	-7.602	-7.864
Ti	1	5766.359	26568.086	55932.777	43901.061	55932.777	1->2	3.0->4.0	1.933	3.019	863.87	0.277	-7.204	-7.540
Ti	1	6085.226	8493.077	64815.472	24922.704	64815.472	0->1	1.0->1.0	1.395	1.658	232.63	0.254	-7.769	-8.270
Ti	1	6085.226	8493.077	68125.805	24922.704	64815.472	0->1	1.0->1.0	1.356	1.658	225.30	0.251	-7.783	-8.179
Ti	1	6121.002	15155.262	63912.060	31488.102	55932.777	0->1	4.0->4.0	1.500	2.118	397.50	0.239	-7.534	-7.786
Ti	1	6497.684	11638.661	55932.777	27027.826	63578.161	0->1	3.0->4.0	1.574	1.732	286.48	0.259	-7.680	-8.271
Ti	1	8518.353	15155.262	63912.060	26890.710	63578.161	0->1	4.0->3.0	1.500	1.729	266.89	0.249	-7.709	-8.332
Ti	1	8778.686	14106.734	64298.963	25495.362	63578.161	0->1	3.0->2.0	1.478	1.697	255.85	0.253	-7.728	-8.466

Spec	Ion	$Wavel$	E_{low}	$E_{limit_{low}}$	E_{upp}	$E_{limit_{upp}}$	L	J	n^*_{low}	n^*_{upp}	σ	α	ABO	$Kurucz$
Si	1	8556.776	47353.138	65747.350	59032.126	66035.000	2->3	2.0->3.0	2.442	3.958	1532.33	0.315	-6.960	-7.357
Si	1	8556.805	49934.130	65747.350	61621.184	66035.000	2->3	3.0->4.0	2.634	4.985	3049.56	0.339	-6.665	-7.140
Si	1	8648.465	50055.114	65747.350	61613.118	66035.000	2->3	4.0->5.0	2.644	4.980	3033.43	0.340	-6.668	-7.141
Si	1	8728.010	49853.474	65747.350	61306.626	65747.350	2->3	2.0->3.0	2.627	4.970	2996.36	0.343	-6.674	-7.142
Si	1	8742.446	47353.138	65747.350	58790.158	65747.350	2->3	2.0->3.0	2.442	3.970	1554.30	0.315	-6.953	-7.353

All the data are in cgs units. Wavelength in cm, energies in cm^{-1}, σ in a_0^2 and L, J and n are the quantum numbers. The columns ABO and Kurucz are also in cgs units.

4.2 Graphs

4.2.1 ABO/Kurucz-ratio plotted against lower energy: Ti

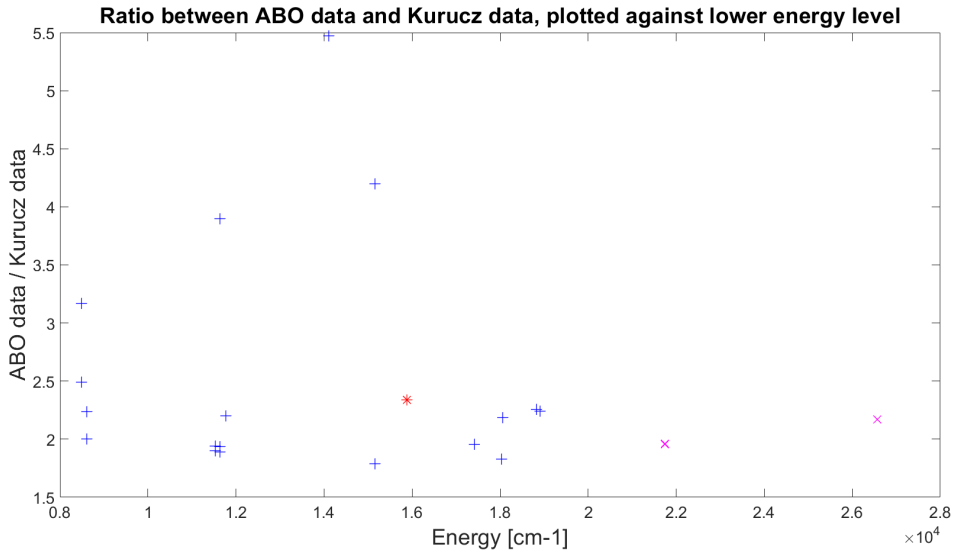

Figure 2: Ratio between ABO data and Kurucz data for a temperature of 10000 K

4.2.2 ABO/Kurucz-ratio plotted against higher energy: Ti

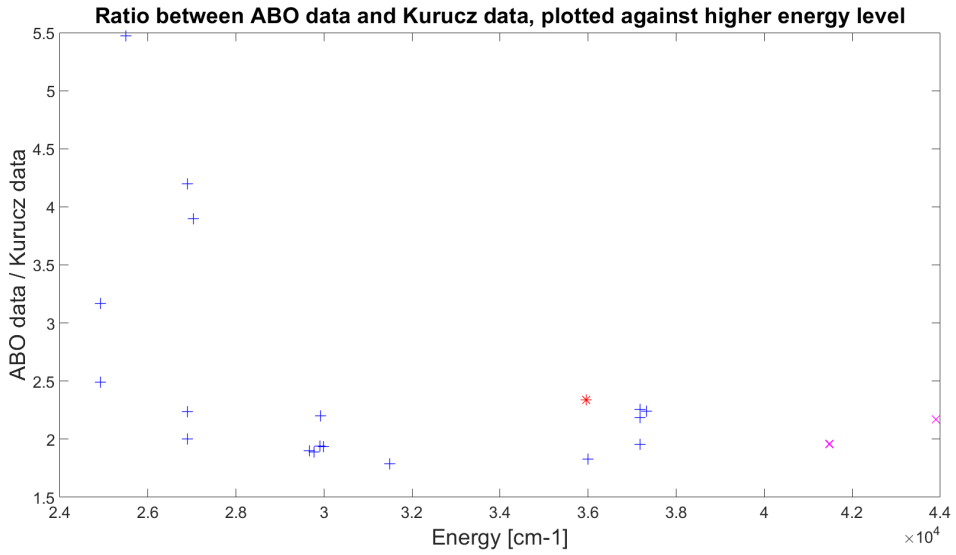

Figure 3: Ratio between ABO data and Kurucz data for a temperature of 10000 K

4.2.3 ABO/Kurucz-ratio plotted against difference in energy: Ti

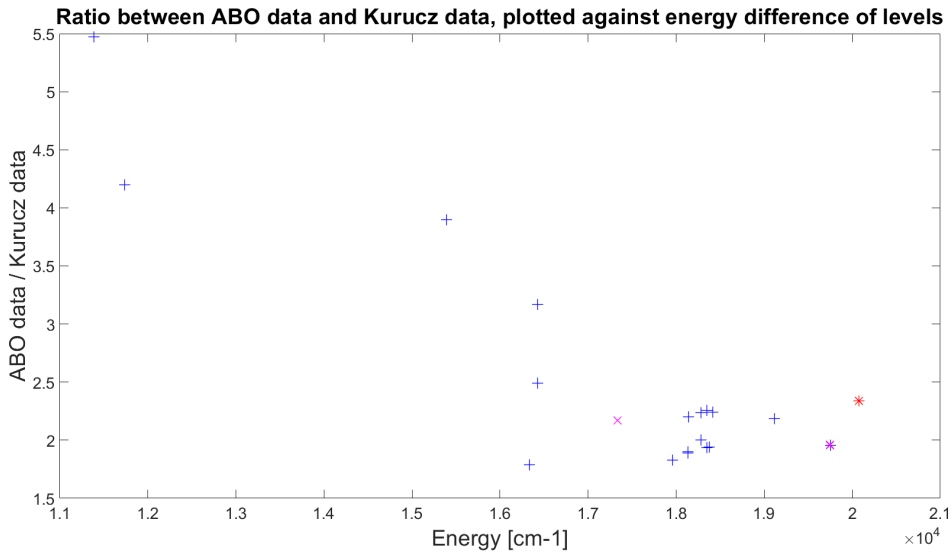

Figure 4: Ratio between ABO data and Kurucz data for a temperature of 10000 K

4.2.4 ABO/Kurucz-ratio plotted against lower energy: Si

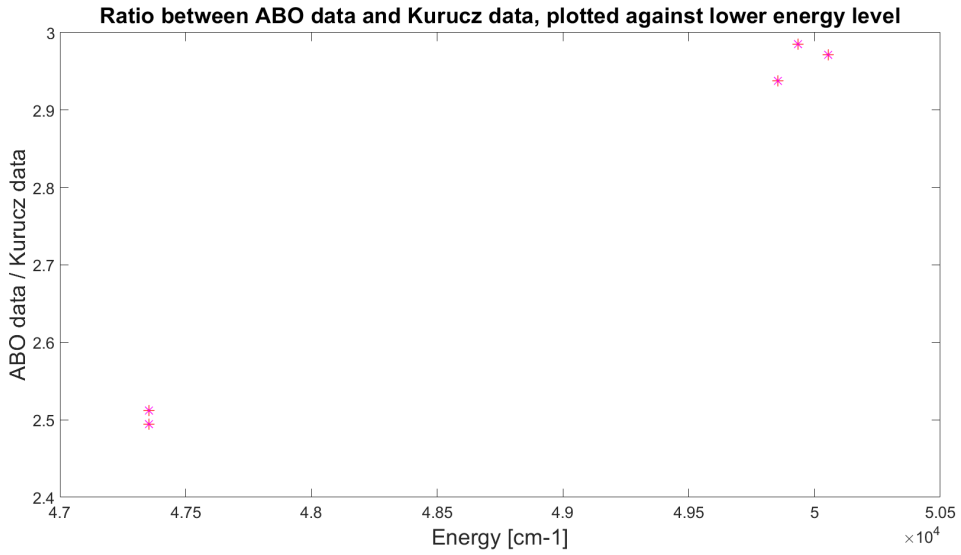

Figure 5: Ratio between ABO data and Kurucz data for a temperature of 10000 K

4.2.5 ABO/Kurucz-ratio plotted against higher energy: Si

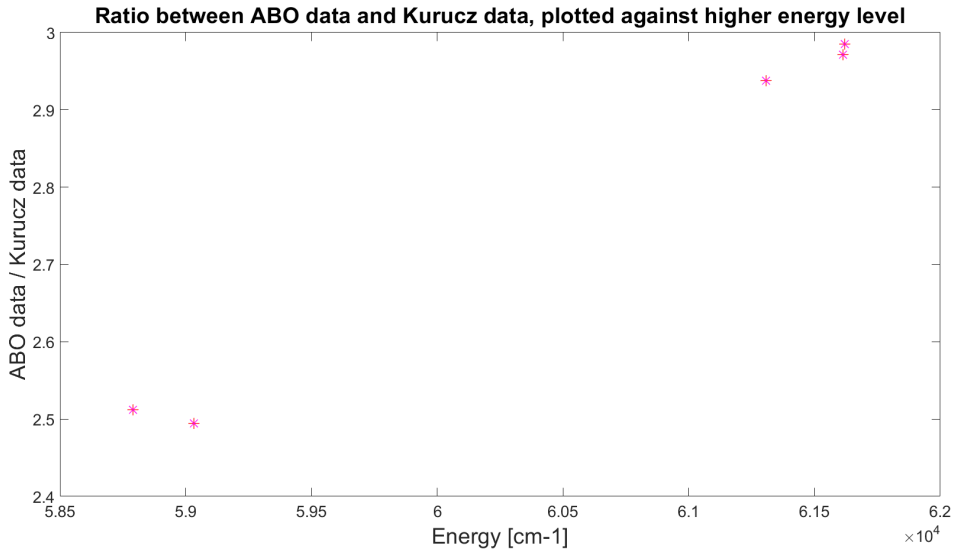

Figure 6: Ratio between ABO data and Kurucz data for a temperature of 10000 K

4.2.6 ABO/Kurucz-ratio plotted against difference in energy: Si

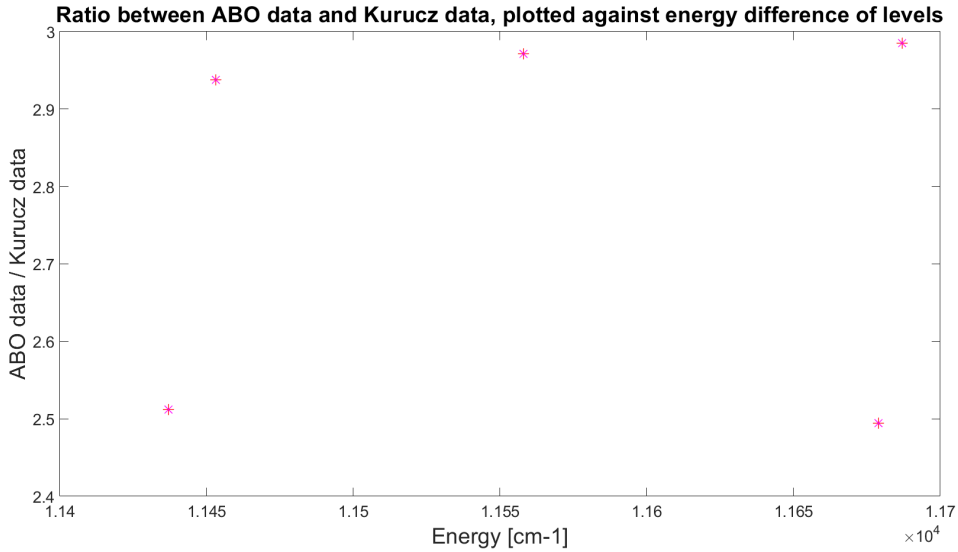

Figure 7: Ratio between ABO data and Kurucz data for a temperature of 10000 K

4.3 Lines not calculated

Out of the 25 lines of titanium 22 were calculated. From the file Ti.out it can be found that the lines not calculated were because of forbidden transitions and because of the results being outside the range of tables. A transition being forbidden means that

$$l \neq \pm 1$$

For the code to work the l has to change by plus or minus one. The other reason means that the tables calculated by (Anstee, S. O'Mara, B, 1995) and (Barklem and O'Mara, 1997) have highest and lowest values for n. If the values calculated is outside that range it is not possible to

make a linear regression. For the silicon this problem was far greater. Out of the 56 lines that were intended to be calculated only 5 were both within the limits and not a forbidden transition. Estimates can be obtained by changing the l for the lower lever such that they are allowed. This introduces some additional errors in the calculations though.

5 Discussion

In figures 2 to 4, the graphs showing the ABO-Kurucz ratio for titanium, the blue cross corresponds to sp-transition, the purple to pd transitions and the red star to the ps transition. For the silicon lines they were all of the type df-transitions.

First, observe the titanium lines, figures 2 to 4. In figure two it can be seen that most of the lines form a horizontal line around 2 on the y-axis. This can be considered a good result since the lines were expected to by roughly twice as large as the previous Unsold data (Bengtsson, K, 2018). There are, however, four points in the data in the range between 3 and 5.5. This is somewhat worrisome since such results were not expected but after checking all their series limits and energies no mistakes could be found. It is worth to note, however, that the four outliers all had fairly low E_{upp}. Though it is not clear how this could cause the difference. Having a small E_{upp} would mean a large binding energy and thus a small $n*_{upp}$ but after checking these number still fell within the boundaries of the tables ($n*_{upp} \approx 1.7$), which shouldn't be low enough to cause trouble.

This behaviour is found in all three graphs for titanium but shows the clearest pattern in figure 3 where they all fall in the lower energies for E_{upp}. The rest of the transitions are all found on virtually the same horizontal line around 2. Sadly, since so many lines were lost it is unclear whether any additional clustering is present in the data. Some of this data could be salvaged by changing the l values as suggested above. This could lend some clues into how the data is structured.

As for silicon, there are clear clusters in figures 5. One lower cluster around 2.5 ABO/Kurucz ratio and the other one just below three. The lower cluster are almost identical transitions, both going from 3s2.3p.3d (1D*') to 3s2.3p.f4 with the only difference being the excitation of the parent configuration in the upper case. They also have the exact same values for J_{low} and J_{upp}.

Likewise for the upper cluster in figure 5 the transitions all share a lot of values. The three all go from 3s2.3p.3d (3F*') to 3s2.3p.5f with differences only in the J quantum number of the configuration. It is also the case for this atom that since so many lines were lost it is hard to show clear patterns in the data. This is an even larger problem for silicon than titanium because there are both fewer lines and only df-transitions.

6 Conclusions

The ABO/Kurucz ration that was expected to be around two, similarly to (Bengtsson, 2018), could be seen for some of the lines but the large number of lines for which data could not be calculated proved to be an issue in drawing definite conclusions about the data. For both titanium and silicon there were clear outliers and it is not obvious how the data could have looked if more lines had been available.

There is, however, some value into knowing that these results were difficult to acquire since it shows which kinds of transitions and materials work better or worse with the ABO theory. There is also a fair amount of the data which does place around a ABO/Kurucz ratio of two.

Before doing similar work in the future it would be wise to first check how much of the data will fall within the "forbidden transitions" territory and if a typical transition is out of bounds or close to. Doing a few of those calculations early on could give indication to how well the data will behave with the ABO cross code.

The method is a powerful tool though, as it gives good results without being overly complicated in its use and could be used on a wide scale for different uses in stellar evolution and abundance.

7 References

Anstee S., O'Mara, B. (1995). Width cross-sections for collisional broadening of s–p and p–s transitions by atomic hydrogen. *Monthly Notices of the Royal Astronomical Society, 276(3), 859 - 866.*

Barklem, PS and O'Mara, BJ. (1997). The broadening of pd and dp transitions by collisions with neutral hydrogen atoms. *Monthly Notices of the Royal Astronomical Society, 290(1), 102 - 106.*

Barklem, PS and O'Mara, BJ and Anstee, SD. (1998). Line broadening cross sections for the broadening of transitions of neutral atoms by collisions with neutral hydrogen. *Publications of the Astronomical Society of Australia, 15(3), 336 - 338.*

Barklem, PS and Piskunov, N and O'Mara, BJ. (2000). A list of data for the broadening of metallic lines by neutral hydrogen collisions. *Astronomy and Astrophysics Supplement Series, 142(3), 467 - 473.*

Kramida, A., Ralchenko, Yu., Reader, J., and NIST ASD Team (2018). NIST Atomic Spectra Database (ver. 5.6.1), [Online]. Available: https://physics.nist.gov/asd [2018, December 26]. National Institute of Standards and Technology, Gaithersburg, MD. DOI: https://doi.org/10.18434/T4W30F

Bengtsson, K. (2018). Broadening of spectral lines in the Gaia-ESO survey (Dissertation). Retrieved from http://urn.kb.se/resolve?urn=urn:nbn:se:uu:diva-355195